Fermi National Accelerator Laboratory

FERMILAB-FN-654

Injection of JHP Main Ring Using Barrier Buckets

King-Yuen Ng

Fermi National Accelerator Laboratory
P.O. Box 500, Batavia, Illinois 60510

January 1997

Operated by Universities Research Association Inc. under Contract No. DE-AC02-76CH03000 with the United States Department of Energy

FN-654
1997

INJECTION OF JHP MAIN RING USING BARRIER BUCKETS

King-Yuen Ng

Fermi National Accelerator Laboratory, P.O. Box 500, Batavia, IL 60510*

(January, 1997)

Abstract

Multiple injections into the 50 GeV proton synchrotron, proposed by the Institute of Nuclear Study of Japan, from a 3 GeV booster using barrier buckets are simulated. For four successive injections of 4 bunches each time, having a half momentum spread of 0.5%, the final coasting beam in the synchrotron has a momentum spread of roughly $\pm 1.0\%$ in the core, with a tail extending up to $\pm 2.5\%$. The choice of debunching time, barrier velocity, barrier voltage, and barrier width is analyzed. Some beam kinematics relating to the barrier buckets are discussed.

*Operated by the Universities Research Association, Inc., under contract with the U.S. Department of Energy.

I. INTRODUCTION

The Main Ring of the Japan Hadron Project (JHP) is a high-intensity fast-cycling synchrotron. The design asks for a ring of 16 bunches with 2×10^{14} protons in total. These 16 bunches are injected from the booster in 4 batches cycling at the rate of 25 Hz. It is possible that the space-charge effect may lead to instability at the injection kinetic energy of 3 GeV. In order to minimize the high space charge, it has been suggested the use of rf barrier waves during the injection [1]. This paper describes a simulation of such an injection. For completeness, some simple formulas for the barrier bucket are derived in the Appendix.

II. CHOICE OF DEBUNCHING TIME

The ring has an imaginary transition gamma of $\gamma_t = 27i$. At the injection kinetic energy of 3 GeV, the slip factor is therefore $\eta = -0.05813$. The injected bunch has maximum fractional momentum spread $\delta = \pm 0.005$. Therefore, for a bunch to debunch until the $\delta = +0.005$ part meets the $\delta = -0.005$ along the phase or time axis, the time required is

$$t_{\text{debunch}} = \frac{T_0}{2|\eta\delta|} = 8.28 \text{ ms} , \qquad (1)$$

where $T_0 = 4.9526$ μs is the revolution time with the ring circumference taken as $C_0 = 1442$ m. We will use $t_{\text{debunch}} = 10$ ms in the simulation.

III. CHOICE OF SQUEEZING TIME

In this simulation, 4 bunches are injected into the ring. Each bunch has 1000 macro-particles distributed randomly in its elliptical envelope in the longitudinal phase space with maximum momentum spread $\delta = \pm 0.005$ and width $\Delta\tau = \frac{1}{17\times 8}T_0$, i.e, the full width is a quarter of the rf wavelength at revolution harmonic $h = 17$. The distribution in the longitudinal phase space is shown in Fig. 1a along with the linear distribution and momentum distributions. Here, the phase axis is measured in time. The bunches are allowed to debunch for 10 ms and the result is shown in Fig. 1b. Two square rf barrier waves are introduced at $\tau = 0$ on the phase axis. One barrier is fixed while the other one moves slowly at the rate of $\dot{T}_2 = -3.884 \times 10^{-5}$ to the right until a space corresponding to four $h = 17$ rf wavelengths or 1.165 μs is opened. The time taken will be 30 ms, so that 40 ms has just elapsed and the next injection of 4 more bunches from the booster is just in time. The situation just after the second injection is shown in Fig. 2a. The procedure then repeats. Debunching in another 10 ms gives Fig. 2b. Introduction of rf barrier waves with squeezing for 30 ms and then the third injection result in Fig. 3a. Another 10 ms of debunching gives Fig. 3b. The next squeezing and the fourth injection result in Fig. 4a. Finally we allow for another 10 ms of debunching before recapturing by the $h = 17$ rf system, and the situation is shown in Fig. 4b. In the above, T_2 is the width of the rectangular part of the bucket. Since the moving barrier pulse squeezes the bucket, $\dot{T}_2 < 0$.

In order that the longitudinal emittance of the bunch inside the barrier bucket is conserved, we must have [2]

$$|\dot{T}_2| \ll \tfrac{1}{2}|\eta\delta| = 1.45 \times 10^{-4} \ . \tag{2}$$

The detail is given in the Appendix. Therefore, the rate of barrier movement chosen in the simulation should be slow enough.

IV. CHOICE OF BARRIER VOLTAGE AND WIDTH

The amount of momentum spread δ_b the pair of square barrier pulses can trap is given by [2]

$$\delta_b = \sqrt{\left(\frac{2}{\beta^2|\eta|}\right)\left(\frac{eV_0T_1}{E_0T_0}\right)} \ , \tag{3}$$

where E_0 is the total energy of the particle and β is velocity relative to the velocity of light. See the Appendix for derivation. Note that the barrier voltage V_0 and barrier width T_1 in Eq. (3) become

$$V_0T_1 \to \int_{\text{barrier}} V(\tau)d\tau \ , \tag{4}$$

when the barrier wave is of arbitrary shape than square. To confine $\delta_b = 0.018$ say, we need

$$V_0T_1 = 173.26 \text{ kV-}\mu\text{s} \ . \tag{5}$$

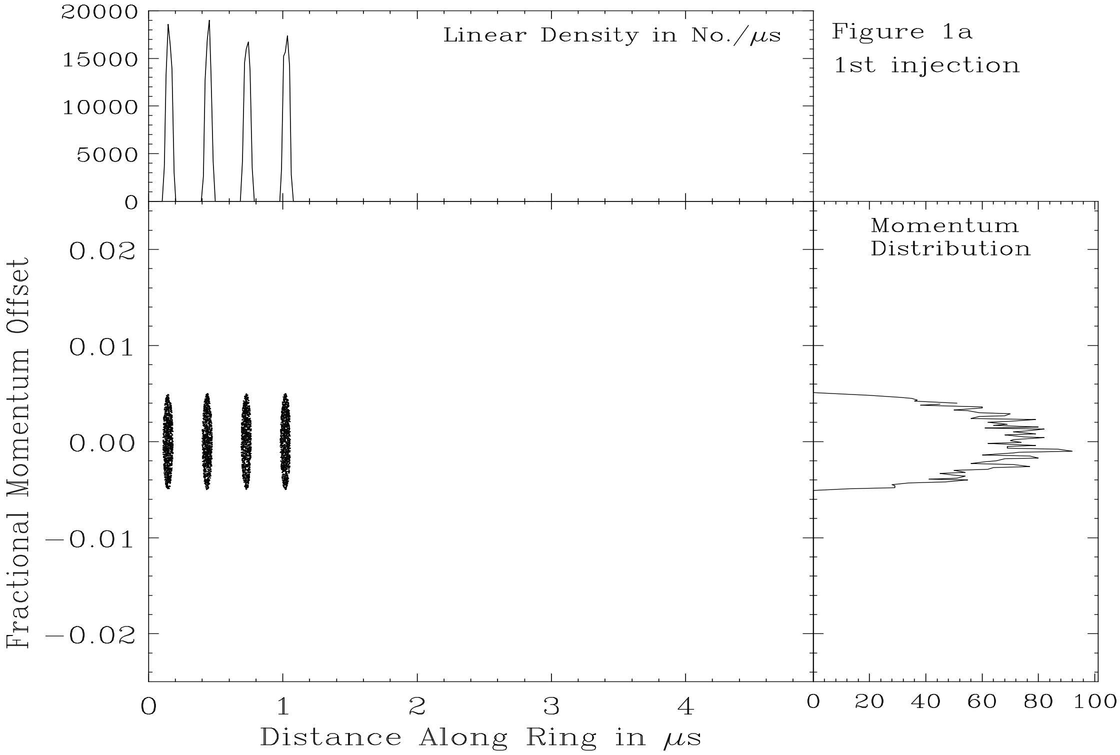
Linear Density in No./μs
Figure 1a
1st injection
Momentum Distribution
Fractional Momentum Offset
Distance Along Ring in μs

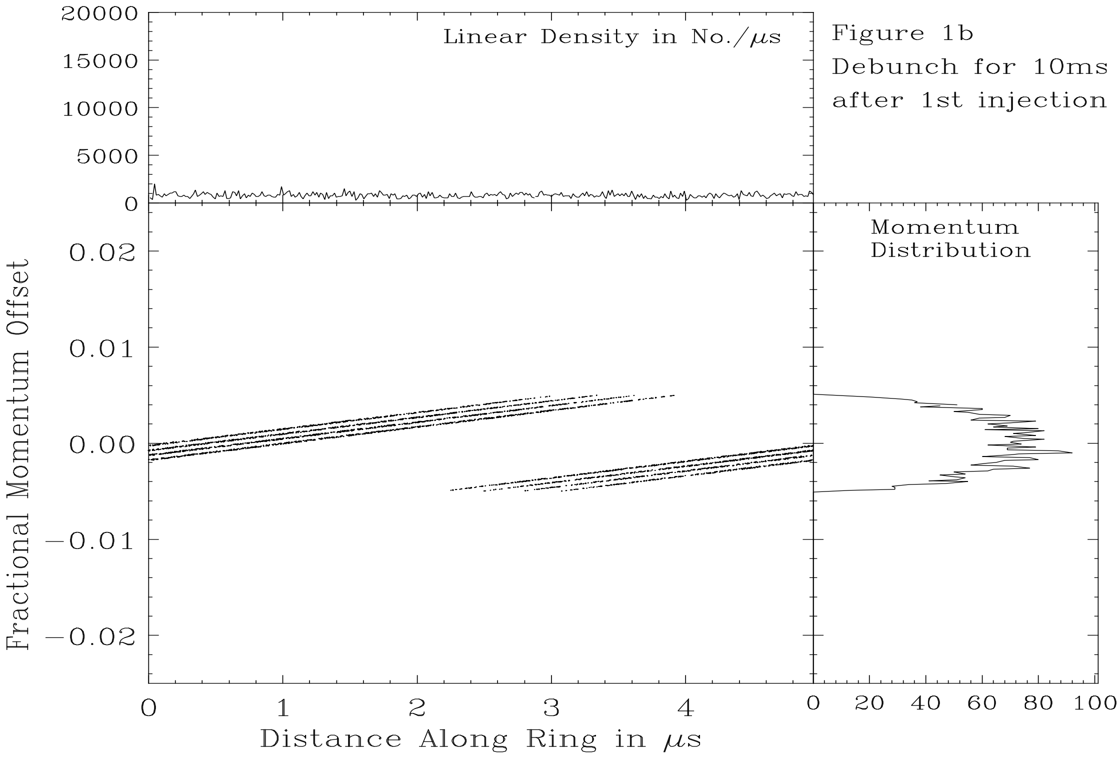
Linear Density in No./μs
Figure 1b
Debunch for 10ms
after 1st injection
Momentum Distribution
Fractional Momentum Offset
Distance Along Ring in μs

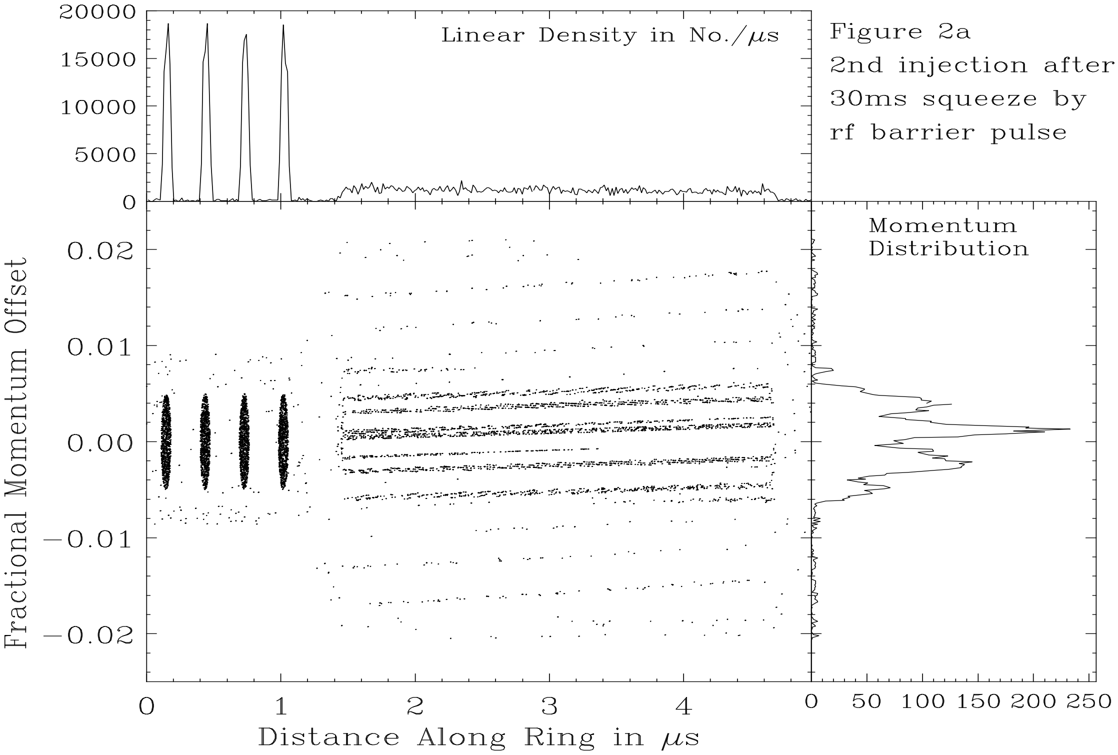

Figure 2a
2nd injection after
30ms squeeze by
rf barrier pulse

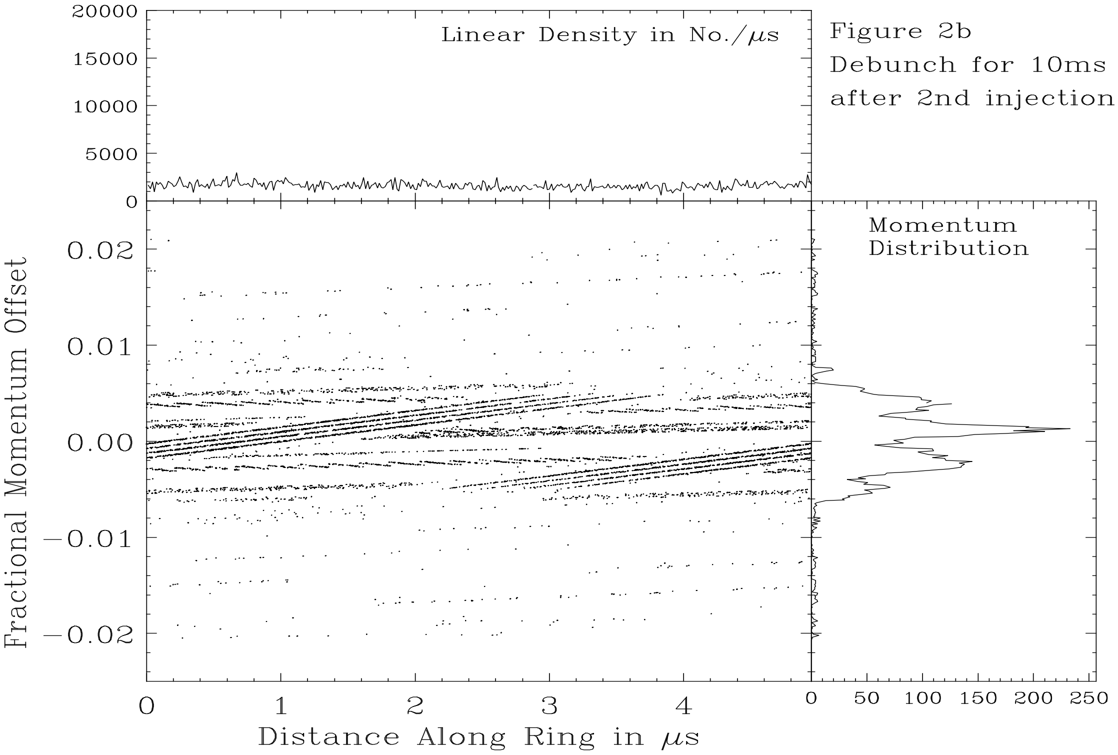

Figure 2b
Debunch for 10ms
after 2nd injection

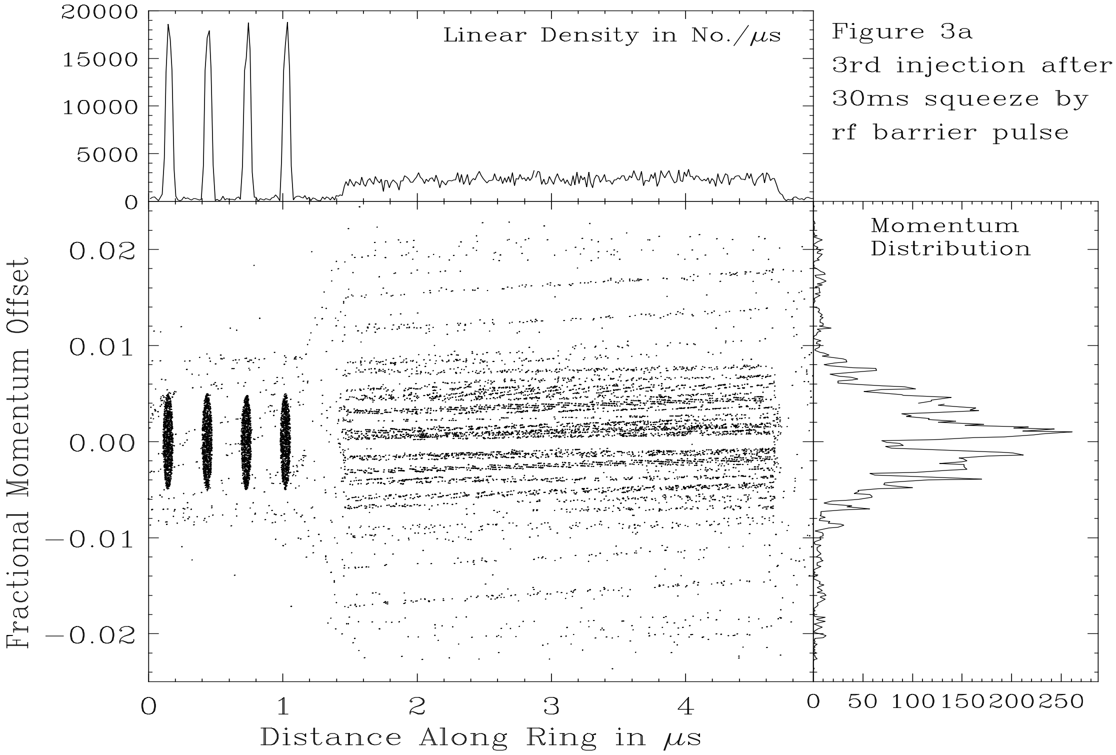

Figure 3a
3rd injection after
30ms squeeze by
rf barrier pulse

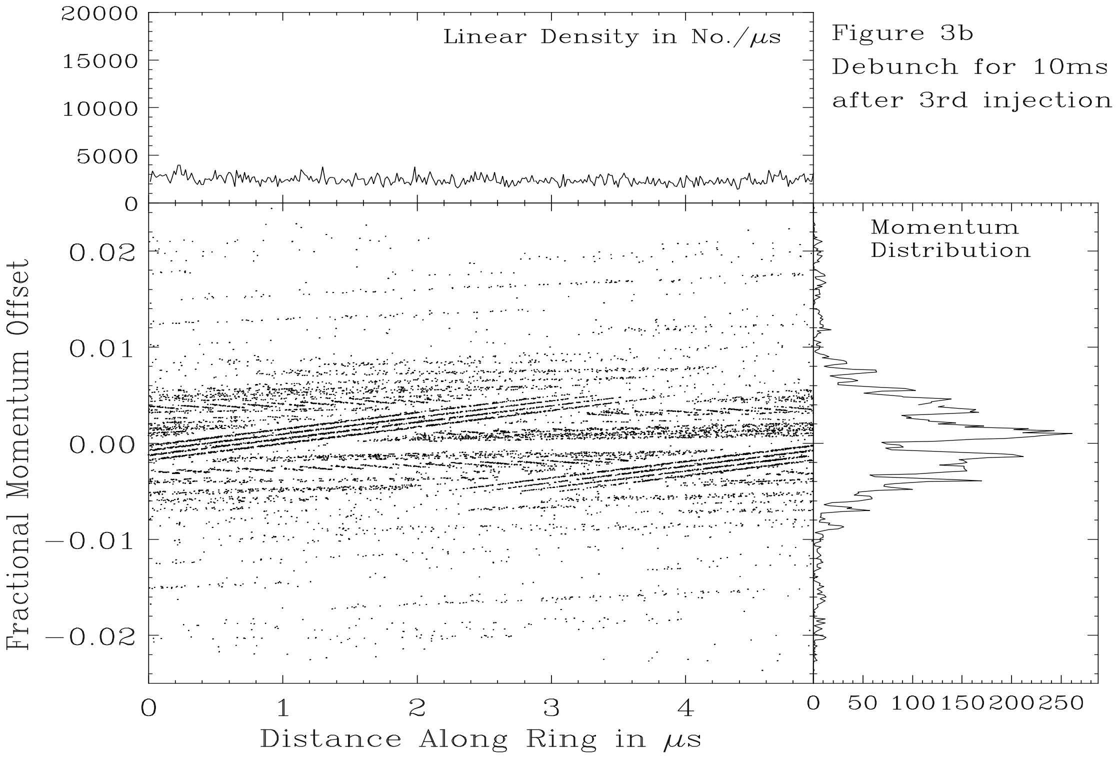

Figure 3b
Debunch for 10ms
after 3rd injection

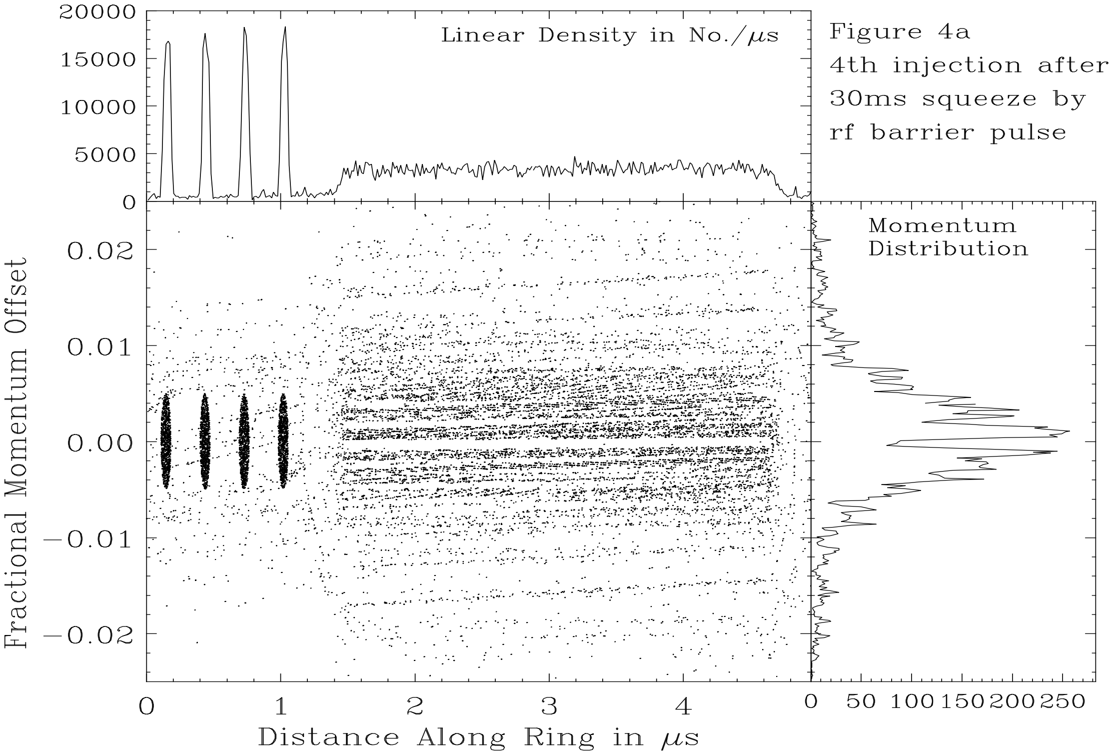

Figure 4a
4th injection after
30ms squeeze by
rf barrier pulse

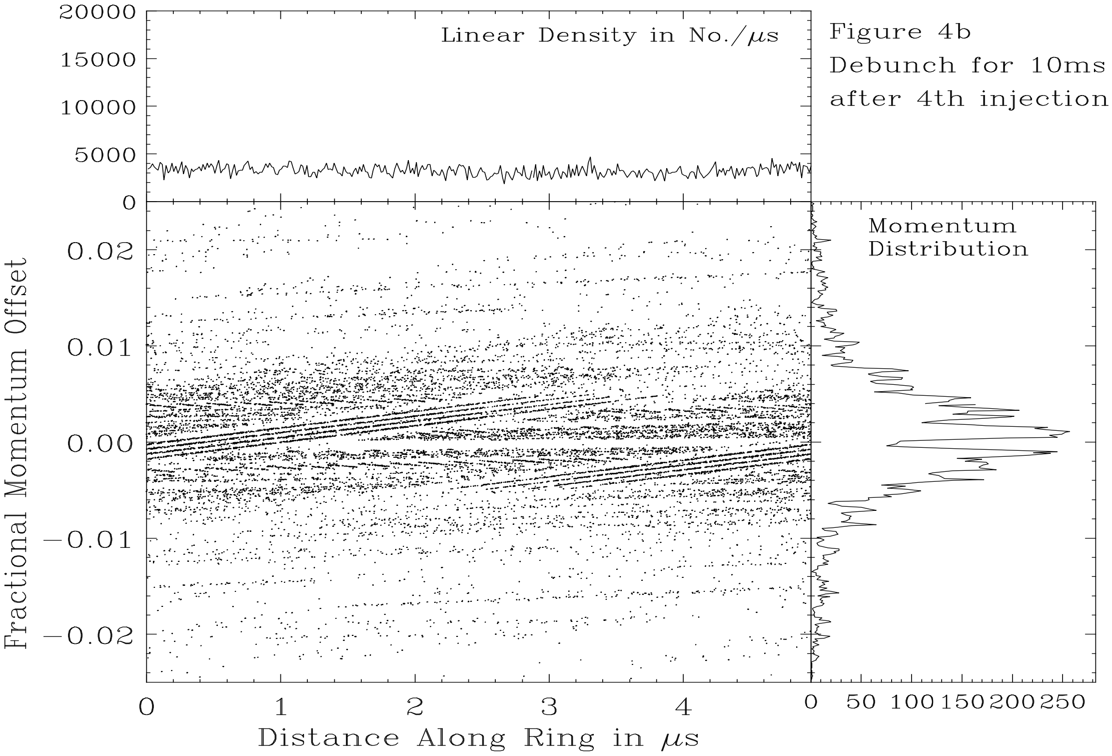

Figure 4b
Debunch for 10ms
after 4th injection

It is not good to use too small a barrier voltage, because this will make the width of the barrier too wide. Remember that the stable bucket consists of a rectangular part where the particles do not see the barrier pulses and two curved parts where the particles are exposed to the barrier voltage. A large barrier width increases the curved parts of the bucket at the expense of the rectangular part, and the whole bucket area becomes smaller. Therefore, when the barrier pulses are switched on, there will be more particles outside the bucket if the barrier pulse width is larger. This is illustrated in Fig. 5. The momentum spread of the eventual phase-space distribution will become larger.

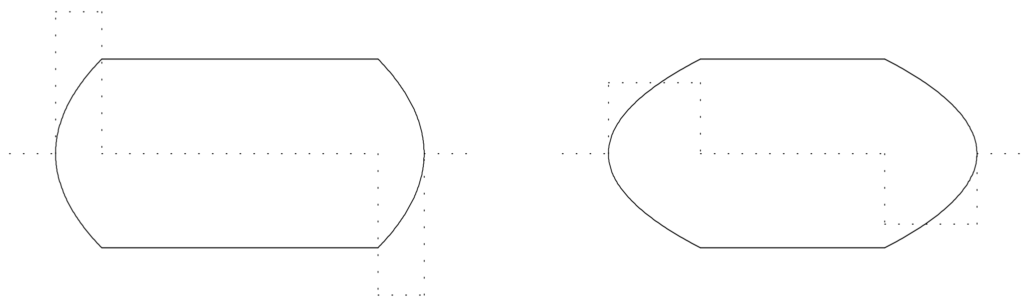

(a) (b)

Figure 5: The barrier pulse voltage V_0 in (b) is one half of that in (a) while the pulse width T_1 is doubled so that $V_0 T_1$ remains constant. This reduces the bucket area although the bucket height remains the same. Therefore, more beam particles will not be captured in case (b).

Too narrow a barrier width is also not desired. This will boost the barrier voltage to too high a value, making it more difficult to generate. Also, whenever a particle drifts towards the barrier, it will gain or lose energy by an amount equal to V_0 per turn, independent of whether the barrier is moving or not. Take an extreme case that the barrier width is so narrow that the particle only sees it in one turn or none at all. If the particle sees the barrier in one turn, it will either gain or lose too much energy that it will be thrown out of the bucket. If the particle misses the barrier, it will also go out of the bucket also. For this reason, in order that the conservation of the area of the square part of the bunch holds, the barrier voltage must be limited to

$$\frac{eV_0}{\beta^2 E_0} \ll \delta_{\rm max} \ , \tag{6}$$

where $\delta_{\rm max}$ is the maximum momentum offset of a particle, and that this particle must see the barrier for a substantial number of consecutive turns. The constraint (6) gives $V_0 \ll 18600$ kV using $\delta_{\rm max} = 0.005$. We actually choose $V_0 = 625$ kV and $T_1 = 0.30$ μs in our simulation. Then, a particle with $\delta = 0.005$ will lose its extra energy in approximately $E_0\delta/(eV_0) = 31.4$ turns and penetrate the barrier by an amount approximately equal to

$$\tau_{\rm penetrate} = \frac{|\eta|\beta^2 E_0 T_0 \delta^2}{2eV_0} = 0.0314 \ \mu{\rm s} \tag{7}$$

These barrier waves can produce a bucket height of $\delta_b = 0.0187$ when $\tau_{\rm penetrate} = T_1$, the barrier width.

V. MOMENTUM-OFFSET DISTRIBUTION

To get an estimate of the momentum spread of most of the particles after each squeezing by the barrier pulse, we neglect the curved part of the barrier bucket. The rectangular part of the bucket has a width of $T_{2\,\rm init} = T_0 - 2T_1$ at the time when the barrier waves are introduced, and becomes $T_{2\,\rm final} = \frac{13}{17}T_0 - 2T_1$ at the end of the squeeze. The momentum spread will be increased by the factor

$$F = \frac{T_0 - 2T_1}{\frac{13}{17}T_0 - 2T_1} = 1.356 \ . \tag{8}$$

Ideally, in the fourth injection after the third squeezing by the rf barrier, the momentum spread should increase only by the factor $F^3 = 2.547$ to $\delta = \pm 0.0127$. We see in Fig. 4a that for most part of the beam, the momentum spread actually increases by such a ratio after 3 barrier squeezes. However there is a small part of the beam having momentum spread as large as $\delta = \pm 0.025$ or even ± 0.030. This is because the above consideration is correct only for a bunch that is initially at equilibrium inside the barrier bucket. Here, the beam particles are *captured* into the barrier bucket when the barrier pulses are turned on. Since we have a debunching before capturing into the barrier bucket, particles can be anywhere along the phase axis at the time of capture. For those particles that are captured into the curved parts of the bucket and are very close to the boundaries of the bucket, they can acquire large amount of energy through the barrier pulses and leave the barrier pulse with much larger momentum offset than the estimate given above. It can be seen in Fig. 1a that there are particles with momentum offsets much larger than $1.356 \times 0.005 = 0.0068$ after the first squeeze by the moving barrier pulse. There are also particles that have not been captured into the barrier bucket at all. For a particle with initial momentum offset $\delta_{i0} > 0$ outside the stable barrier bucket, it will first drift across the moving barrier pulse and result in a momentum offset of δ_{f1} given by

$$\left(\delta_{f1} + \frac{\dot{T}_2}{|\eta|}\right)^2 = \left(\delta_{i0} + \frac{\dot{T}_2}{|\eta|}\right)^2 + \delta_b^2 \ , \tag{9}$$

where $\dot{T}_2$ is negative (see Appendix). The particle then drifts across the stationary barrier pulse to the space opened up by the moving barrier, after making synchrotron drifting once around the ring. The momentum offset will be reduced to δ_{i1} with

$$\delta_{f1}^2 = \delta_{i1}^2 + \delta_b^2 \ . \tag{10}$$

Since the initial momentum offset is at most $\delta_{i0} = 0.005$, during the first synchrotron *rotation* (not oscillation or libration) outside the barrier bucket, we have therefore $\delta_{f1} = 0.0194$ and $\delta_{i1} = 0.0067$. This is illustrated in Fig. 6. On the average, this particle will encounter the moving barrier pulse 4 times during the 30 ms squeeze time. At the end of the first squeeze, we have $\delta_{f4} = 0.0206$. After that there is another 10 ms of debunching and some of these large-momentum-offset particles can land outside the barrier bucket again when the next barrier pulses are turned on. Thus, for the second squeezing, there may be particles having $\delta_{i0} = 0.0206$ to start with. At the end of the second squeeze after another 4 encounters with the moving barrier pulse, we obtain $\delta_{f4} = 0.0282$ by solving again Eqs. (9) and (10). Continuing on in this way to the end of the third squeeze, we will have some particles with the largest momentum offset of $\delta_{f4} = 0.0340$. When we analyze the momentum distribution in Fig. 4a more carefully, we do find 18 particles out of 16,000 in the momentum-offset range of 0.025 to 0.030, and 1 particle in the range of 0.030 to 0.035.

The above analysis depends on the time-integrated barrier voltage only and is independent of the barrier voltage itself. However, if we use a higher barrier voltage

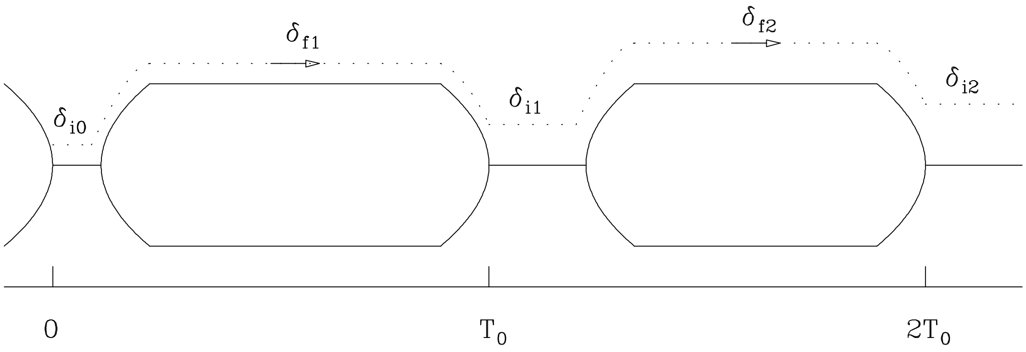

Figure 6: The Poincaré trajectory of a particle outside the barrier bucket. With one barrier pulse (the left one in the bucket) moving to the right, the momentum offset increases for every synchrotron *rotation* around the ring, whose circumferential length in time is T_0.

while keeping $V_0 T_1$ constant, more particles will be captured into the larger stable barrier bucket, although the bucket height will remain the same. Thus, the probability of having particles to attain large momentum offset outside the bucket will become smaller. Moreover, because the larger barrier voltage increases only the rectangular area of the bucket but not the bucket height as indicated in Fig. 5, the bunch area that has momentum offset within $\delta = \pm 0.005$ (for the first injection) and fits the bucket will be relatively larger. Thus not so many beam particles will attain higher momentum offsets via synchrotron oscillations. When one of the barrier pulse moves, more particles will follow the momentum-offset increase governed by Eq. (8). To demonstrate this, we perform a similar simulation by doubling the barrier voltage to $V_0 = 1250$ kV while halving the barrier width to $T_1 = 0.15$ μs. The phase space distribution after three squeezes is shown in Fig. 7. Comparing with Fig. 4a, we do see less particles land at larger momentum-offsets, which is verified also numerically by Table I. However, as was pointed out in the previous section, too high a barrier voltage is not desired.

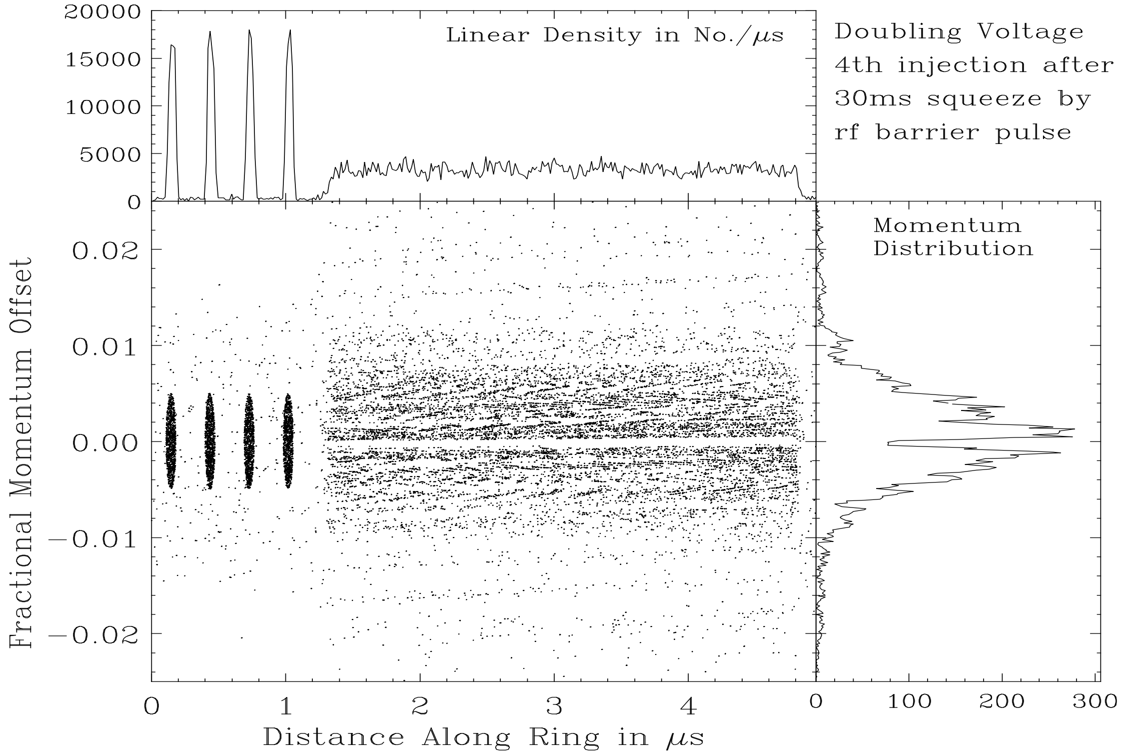

Figure 7: Phase space distribution after 3 barrier squeezes and 3 injections. Compare with Fig. 4a, the voltage of barrier pulses have doubled to $V_0 =$ 1250 kV and the width halved to $T_1 = 0.15$ μs.

VI. DISCUSSIONS

1. Bunch width at injection

Although the simulation results depend very strongly on the momentum spread of the bunches at injection, however, they are very insensitive to the bunch length at injection. This is because there is always a debunching period before a squeeze by the barrier pulse, and the information of the bunch length disappears after debunching. In practice, however, the initial bunch length cannot be too long, because some gaps must be provided for the kicker rise and fall times. In the above simulations, the total bunch length is $\frac{1}{4}$ of a $h = 17$ rf wavelength. Thus the space between the end of the squeezed barrier bunch and the first bunch in the next injection is $\frac{3}{8}$ of a $h = 17$ rf wavelength, or 109 ns. There will be a gap of similar length between the fourth

Table I: Comparison of momentum-offset distributions after 3 squeezes using single barrier pulses of 625 and 1250 kV (first and second columns) and double pulses of 625 kV (last column).

Range of Momentum-offset	Fraction of Particles		
	$V_0 = 625$ kV	$V_0 = 1250$ kV	double 625 kV
0.000 to 0.005	0.6673125	0.7241875	0.650875
0.005 to 0.010	0.2133750	0.2041875	0.188625
0.010 to 0.015	0.0642500	0.0396250	0.058750
0.015 to 0.020	0.0387500	0.0224375	0.044500
0.020 to 0.025	0.0151250	0.0092500	0.042500
0.025 to 0.030	0.0011250	0.0003125	0.011625
0.030 to 0.035	0.0000625	0.0000000	0.003000
0.035 to 0.040	0.0000000	0.0000000	0.000125

bunch and the front of the squeezed barrier bunch. These gaps will be long enough for the injection, because, for example, the kicker of the Fermilab Main Ring has rise and fall times of only $\sim$ 30 ns. Even if the injection bunch length is doubled, these gaps are still 73 ns wide and are wide enough for the injection.

2. Double barrier pulses

Instead of using one negative pulse and one positive pulse to set up the barrier bucket and perform the bunch squeezing, we may utilize instead a pair of identical double pulses. Each double pulse consists of a positive voltage V_0 of duration T_1 followed by a negative voltage $-V_0$ of duration T_1. Instead of square waves, each pulse can be one sinusoidal period of an rf wave. At switch-on, the two pulses overlap each other. Then, one pulse moves to the right while the other one remains stationary. Under this situation, the space opened up by the moving pulse also forms a stable barrier bucket via the negative half of the moving pulse and the positive half of the stationary pulse. Thus some particles will be trapped there and they will have their momentum offsets decreased gradually, because this bucket is becoming wider and wider now as one of the barrier pulses moves to the right. These particles will not be able to drift to the squeezed beam region to acquire larger momentum offsets.

However, there are disadvantages also. The particles that are trapped in the space opened by the moving barrier can be lost when the kicker is fired for the next injection. Also, stable barrier bucket only starts to form after the moving barrier moves a distance of T_1. Before that, the two barrier pulses overlap at least partially. At switch-on, the two barrier pulses overlap completely; i.e., an equivalent pulse height of $2V_0$ width T_1 followed by pulse height of $-2V_0$ width T_1. The barrier bucket forms at this moment will have a bucket height $\sqrt{2}\delta_b = 0.0257$ instead, where δ_b is the bucket height when single barrier pulses are used. Thus particles will bound off from the barriers having much larger momentum offsets. A simulation has been performed with the double barrier pulses using $V_0 = 625$ kV and $T_1 = 0.30$ μs. The phase space distribution after the third squeeze and fourth injection is shown in Fig. 8. We can actually see the two stable barrier buckets, each having a bucket height of ~ 0.025. Comparing with Fig. 4a, we see that the momentum distribution spreads out wider. The fractional populations for some momentum-offset ranges are also listed in the last column of Table I for comparison.

3. Pros and cons of the method

There are pros and cons for using the barrier pulses in multiple injections. The advantage is obviously the much shorter exposure duration of bunches of very high linear intensity to the vacuum chamber, and we hope that no collective instabilities would develop during this shorter duration. For the simulation illustrated in Figs. 1 to 4, the linear line density has been reduced by a factor of ~ 6. This reduction will be more significant if the bunch width at injection becomes narrower. The disadvantage is that microwave instability can develop during debunching when the local momentum spreads of the debunched bunches become small enough. Also, because of the introduction of the barrier pulses and the movement of one of them sends quite a number of beam particles to large momentum offsets, the momentum spread of the final beam will become much larger. Finally, there must be another recapturing of the beam particles into the $h = 17$ rf buckets for acceleration. Beam loss will become inevitable during the recapturing. Thus, there will be beam loss as well as emittance blowup during the whole procedure, which may or may not be tolerable.

Another method is to lengthen the bunches in the booster and perform simple

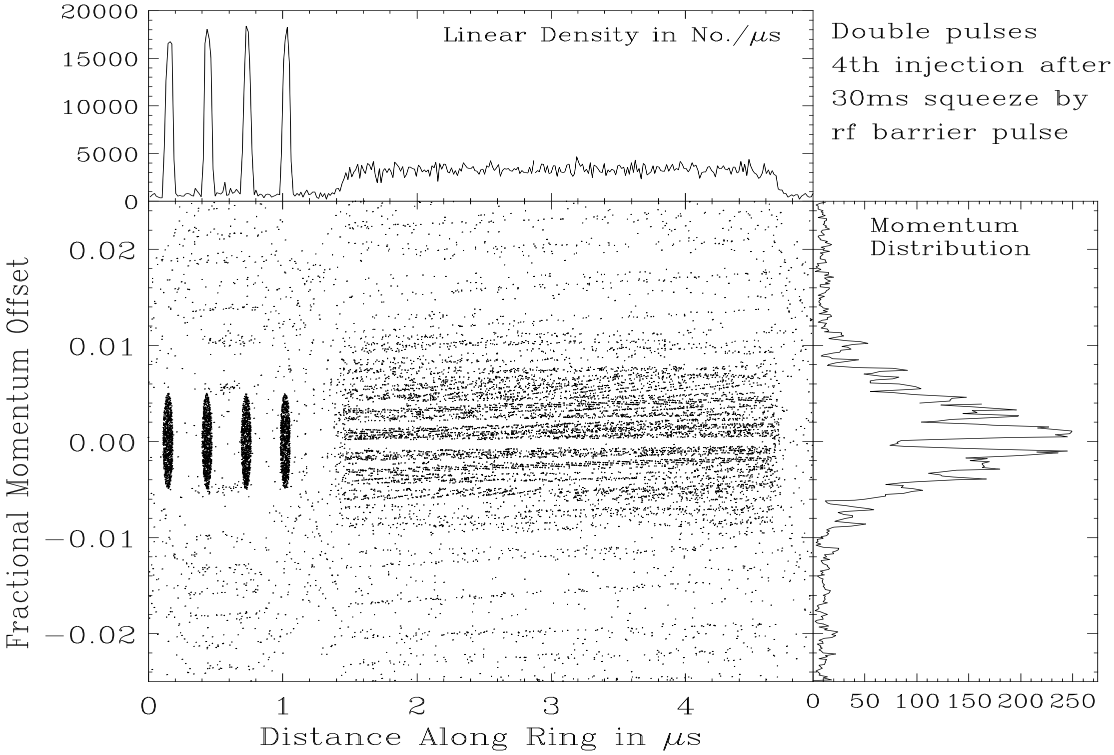

Figure 8: Phase space distribution after 3 barrier squeezes and 3 injections. Compare with Fig. 4a, two double barrier pulses are used at each stage. The pulse height remains $V_0 = 625$ kV and each half of each double pulse has the same width $T_1 = 0.3$ μs.

bucket-to-bucket injection into the main ring. For example, if each bunch is lengthened to occupy 80% of the $h = 17$ bucket with the momentum spread unchanged, the gap between two consecutive bunches becomes 58 ns and is still long enough to accommodate the kicker rise or fall time. This bunch lengthening will introduce a reduction of the local linear density by a factor of 3.2 already compared with the factor of 6 in the simulation. Of course, such a bunch lengthening can be accomplished by a bunch rotation in the booster with negligible emittance increase. In this way, the momentum offset will be smaller and the eventual bunch-to-bunch injection will become easier. Since no recapturing will be necessary, the beam loss during injection can be kept to a minimum.

APPENDIX

A Bucket Height

Choosing time τ and momentum offset δ as the canonical variables, the Hamiltonian of a particle in the *stationary* barrier-wave system can be written as

$$H = \frac{1}{2}\eta\delta^2 + \frac{1}{\beta^2 E_0 T_0}\int_0^\tau eV(\tau')d\tau' \ , \tag{A1}$$

where the first term is the 'kinetic energy' of the particle and the second term is 'potential energy' due to the barrier pulse, which has been chosen to be zero inside the bucket away from the barrier. For square barrier pulse at the right side, the integral just gives $-V_0\tau$. The bucket height δ_b is therefore given by equating the maximum kinetic energy to the maximum potential energy,

$$\frac{1}{2}|\eta|\delta_b^2 = \frac{eV_0T_1}{\beta^2 E_0 T_0} \ , \tag{A2}$$

which gives Eq. (3).

B Synchrotron Period

A particle drifts along most of the time giving the rectangular part of the barrier bucket and sees the barrier pulses very briefly giving the curved parts of the bucket. If we neglect the short excursion time of the particle into the curved part of the bucket, the synchrotron period is just the drifting time along a length $2T_2$ of the phase axis; i.e.,

$$2T_2 \approx T_{syn}|\eta|\hat{\delta} \ . \tag{A3}$$

Here T_2 is roughly between $\frac{13}{17}T_0$ and T_0. Thus, for a particle with maximum momentum offset $\hat{\delta} = 0.005$, the synchrotron period is $T_{\rm syn} \approx 26$ to 34 ms. Or the particle makes only one synchrotron oscillation during the barrier squeezing time of 30 ms, and there are at the most two encounters with the moving barrier pulse. For a particle with maximum momentum offset of $\hat{\delta} = 0.020$, the synchrotron libration period or rotation period is $T_{\rm syn} \approx 6.5$ to 8.5 ms, and the particle will encounter the moving barrier about 4 times.

C Moving Barrier Pulse

When a particle with momentum offset δ_i hits a *stationary* barrier pulse, it will reverse its direction and come back with momentum offset $\delta_f = -\delta_i$ as shown in Fig. 9a. Here we assume that the barrier voltage $\pm V_0$ is small enough so that the

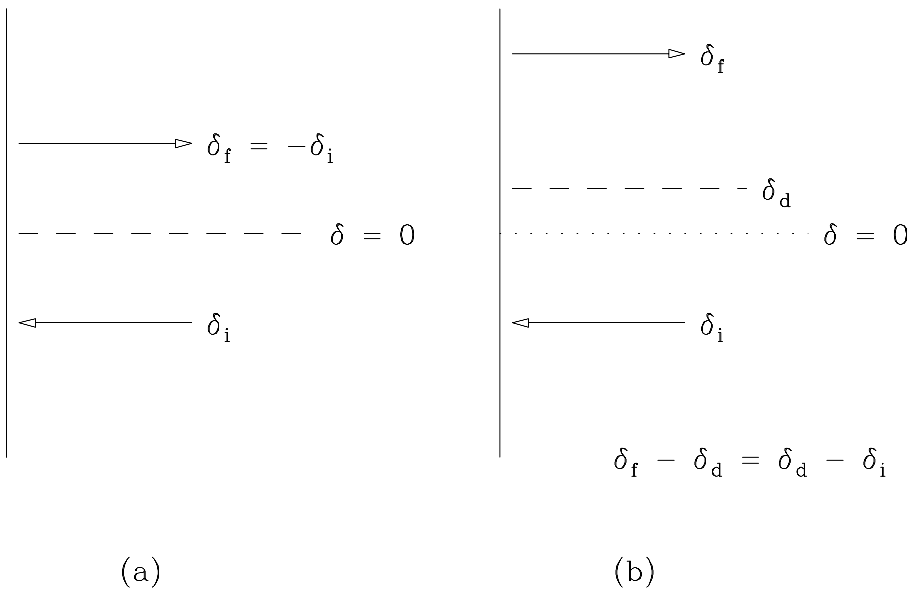

Figure 9: (a) A particle with momentum offset $\delta_i < 0$ encounters a stationary barrier pulse resulting in momentum offset $\delta_f = -\delta_i$. The stationary barrier pulse considers those on-momentum particles as at stable fixed points. (b) The barrier pulse moves at the drifting speed of particles with momentum offset δ_d and considers these particles as at stable fixed points. A particle with momentum offset $\delta_i < 0$ encountering the moving barrier pulse will have its momentum offset changed to δ_f so that $\delta_f - \delta_d = \delta_d - \delta_i$.

particle sees the square pulse for a substantial number of successive turns and the momentum change for the particle per turn is small, or

$$|\Delta\delta| \ll \frac{eV_0}{\beta^2 E_0} \ . \tag{A4}$$

For those particles with $\delta = 0$ inside the barrier bucket, this barrier considers them to be stationary. In other words, these particles are at the stable fixed points (in fact, a whole line inside the rectangular part of the bucket). Now consider this barrier pulse moving to the right at a rate of $\dot{T}_2 < 0$. Particles with momentum offset

$$\delta_d = \frac{|\dot{T}_2|}{|\eta|} \tag{A5}$$

are drifting at the same rate as the barrier. In the point of view of the moving barrier, these particles are at the stable fixed points, because they appear to be stationary to the moving barrier. Therefore, a particle with momentum offset $\delta_i > \delta_d$ drifts faster than the moving barrier and will not encounter it at all. On the other hand, a particle with momentum offset $\delta_i < \delta_d$ will be turned back by the moving barrier with momentum offset δ_f given by

$$\delta_f - \delta_d = \delta_d - \delta_i \tag{A6}$$

as is indicated in Fig. 9b. This can be verified easily if we go to the rest frame of the moving barrier.

If the bunch has a maximum momentum spread $\hat{\delta} < \delta_d$ initially, there will not be any particle supply to the region $\hat{\delta} < \delta < \delta_d$ in the longitudinal phase space, which will become empty after the squeezing motion of the moving barrier, as shown in Fig. 10. Although Liouville theorem guarantees the preservation of particle density, the longitudinal bunch emittance will be increased eventually due to filamentation.

Moreover, not all the particles in the bunch will complete exactly a half integral number of synchrotron oscillations in a certain time interval, even if $\hat{\delta} > \delta_d$ to start with, the edge of the bunch will be left uneven as indicated in Fig. 11. Eventually, the longitudinal bunch emittance will be increased also. Thus, to preserve bunch emittance, we require the change of momentum spread at each encounter with the moving barrier to be small. More precisely, using Eq. (A6), we require

$$2\delta_d \ll \hat{\delta}\ , \tag{A7}$$

which leads to Eq. (4).

For a particle with momentum offset $\delta_{f1} > \delta_b$ outside the barrier bucket set up by stationary barrier pulses, it will acquire a potential energy of $-eV_0T_1/(\beta^2E_0T_0)$ after crossing the barrier at the right side, and the momentum offset δ_{i1} will become

$$\frac{1}{2}\eta\delta_{f1}^2 = \frac{1}{2}\eta\delta_{i1}^2 - \frac{eV_0T_1}{\beta^2E_0T_0}\ , \tag{A8}$$

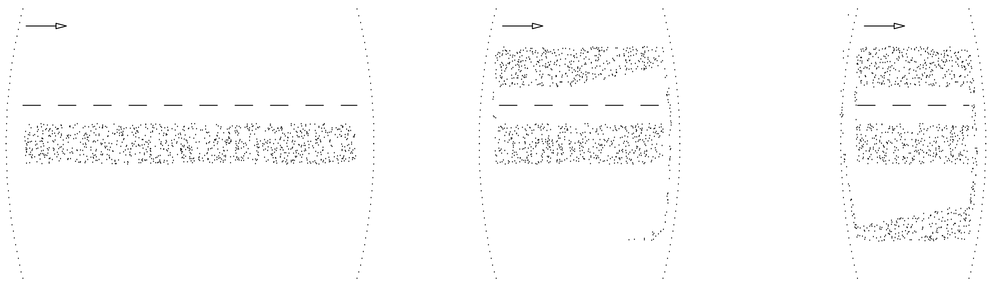

(a) (b) (c)

Figure 10 : Particles inside a narrowing barrier bucket. The left-side barrier pulse moves at the drifting speed of particles represented by dashed lines. (a) Initially, the bunch has momentum spread larger than these particles. As the bucket is squeezed to (b) and (c), empty spaces develop. Some particle loss is seen in (c).

where the Hamiltonian of Eq. (A1) has been employed. Using the definition of the bucket height δ_b in Eq. (A2), we obtain immediately the relation,

$$\delta_{f1}^2 = \delta_{i1}^2 + \delta_b^2 \ . \tag{A9}$$

For a barrier pulse moving at the rate of $\dot{T}_2$, Eq. (A9) applies in the rest frame of the moving barrier. Equivalently, $|\dot{T}_2|/|\eta|$ has to be subtracted from δ_{f1} and δ_{i1}, which results in Eq. (9).

One may notice that there is always a dip in the central region of the momentum distribution curves. This is because after each debunching period, for example in Fig. 1b, the only particles with small momentum offsets reside on the very left side of the phase axis. For momentum offsets that are slightly positive, these particles will continue to spread out to the right and fill up the whole phase axis, after moving barrier is turned on later. For momentum offsets that are slightly negative, however, the particles drift to the left and will be intercepted by the moving barrier very soon. From the above discussion, it is easy to see that there will not be any new supply of particles to this momentum region by reflection via the barrier pulses. For this reason, there is always a dip in this momentum region in all the momentum distribution curves at the place where the momentum offset is slightly negative..

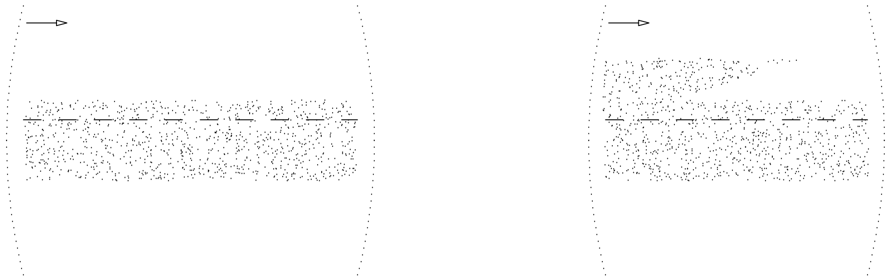

(a) (b)

Figure 11: Particles inside a barrier bucket that is being squeezed. The left-side barrier pulse moves at the drifting speed of particles represented by dashed lines. (a) Initially, the bunch has momentum spread larger than these particles. However, because not all particles complete a half integral number of synchrotron oscillations, the edge of the bunch in (b) becomes uneven.

References

[1] Some preliminary simulations have been performed at the Institute of Nuclear Study of Japan.

[2] S.Y. Lee and K.Y. Ng, *Particle dynamics in storage rings with barrier rf systems,* 1996, to be published in Phys. Rev. **E**.